# Low-Temperature Fluorination of Silica by a Nonaqueous Solution of $NH_4F$

**R. M. Barabash,[†] V. N. Zaitsev,[†] T. V. Kovalchuk,[‡] H. Sfihi,[§] and J. Fraissard*[,‡]**

*Taras Shevchenko National University, Department of Chemistry, 60, Volodymyrska Str., 04030 Kyiv, Ukraine, E.S.P.C.I., Laboratoire SIEN Physique Quantique, CNRS-FRE 2312, 10, rue Vauquelin 75005 Paris, France, and Université Pierre et Marie Curie, case 196, Laboratoire SIEN, Chimie des Surfaces, CNRS-FRE 2312, 4, Place Jussieu, 75252 Paris Cedex 05, France*

*Received: August 14, 2002; In Final Form: April 1, 2003*

The fluorination of silica by ammonia fluoride in several organic solvents has been studied by diffuse reflectance Fourier transform infrared spectroscopy with in situ thermal treatment, $^{19}F$ magic angle spinning nuclear magnetic resonance, $^{1}H \rightarrow {}^{29}Si$ and $^{19}F \rightarrow {}^{29}Si$ cross-polarization techniques, and temperature-programmed analysis followed mass spectrometrically. The extent of surface fluorination and the type of fluorinated species depend on the solvent and treatment procedure. The silicas that were studied show evidence of the formation of two types of surface-fluorinated silicon species: suface-bonded tetrahedral species with a general formula of $O_n$-$Si(OH)_{4-n-m}F_m$ and, to a lesser extent, octahedral species $[F_nSi(OH)_{6-n}]^{2-}$, which were formed already at low temperature. The thermal decomposition of $[F_nSi(OH)_{6-n}]^{2-}$ leads to the removal of corresponding silicon fluorides and hydroxyfluorides, and surface-bonded $O_3Si-F$ and $O-SiF_3$ can be additionally formed. Heating to 500−600 °C causes the surface migration of fluorine in $O_3Si-F$ over siloxane bridges and the formation of silicon fluorides and their subsequent removal from the surface (complete removal at 600 °C). The hydrophobic nature of fluorinated silica has been shown by infrared spectroscopy and by the thermal dependence of water desorption from the surface.

## 1. Introduction

When oxide materials are used as catalysts, surface hydroxyls or water possibly present in reaction media may cause serious problems, especially when high acidity is desirable, as in *n*-alkane isomerization. Materials based on silica with various covalently bonded groups are often used as heterogeneous environmentally friendly catalysts.[1−3] However, because of steric hindrance, complete conversion of surface hydroxyls cannot be achieved.[1] Low acidity of residual silanols decreases the overall acidity of the catalyst and increases its hydrophilic nature. To overcome these drawbacks, the replacement of surface Si−OH groups with Si−F can be proposed.[4−6] In addition to the rise in catalyst acidity and activity, for example, in cumene cracking,[4] such replacement improves the hydrophobic properties of the carrier.[7] The known procedure of fluorination includes $SiO_2$ treatment with an aqueous solution of $NH_4F$ or KF with subsequent calcination at high temperatures[5,6,8] and thus cannot be applied to silica with covalently immobilized organic groups because the organic layer would be destroyed and the silica would be contaminated by water. Alternative fluorination of silica with HF in nonaqueous media results in the formation of a HF−silanol coordination complex, and further calcination at 450 °C is required to achieve Si−F bond formation.[7] Herein we report the attempt to develop the low-temperature fluorination of silica using aqueous solutions, nonaqueous solutions, or mixed water−organic solutions of $NH_4F$. To study the effect of the solvent, the fluorination reaction is carried out in $CH_3$-CN, ethylene glycol, propylene carbonate, and a water−*tert*-butyl alcohol mixture. An important objective is to avoid excessive fluorination leading to the octahedral $SiF_6^{2-}$ species because of subsequent surface erosion and catalyst destruction.[8] As shown by Duke et al.,[8] the fluorination of silica by aqueous KF or $NH_4F$ leads to the formation of surface $O_3Si-F$ bonds and $SiF_6^{2-}$ anions. Later, Clark et al.[9] proposed that the treatment of silica with different fluorinating reagents in aqueous solution may lead to the formation of various $(F_nSi(OH)_{6-n})^{2-}$ species rather than simply $SiF_6^{2-}$ anions, although the fluorination is somewhat dependent on the type of reagent used and the experimental conditions. Heating causes the evolution of complex hydroxyfluorides and the formation of residual tetrahedral $O_3Si-F$ species.

In our study, we attempt to follow and compare aqueous and nonaqueous fluorination and to characterize the nature of the fluorinated silica surface by means of physical methods such as diffuse reflectance Fourier transform infrared spectroscopy (DRIFT) and magic angle spinning nuclear magnetic resonance with cross polarization (CP-MAS NMR). Programmed thermal desorption followed with the use of mass spectrometry (TPD MS) is employed to study the stability and hydrophobicity of the fluorinated surface and the thermal behavior of surface fluorinated species.

## 2. Experimental Section

Two silica precursors, pyrogenic silica (Stavropol 120), referred to as silochrome and denoted SC, and precipitation silica (Zeosil, Rhone-Poulenc), referred to as zeosil and denoted Zs, were chosen. This choice of different silica precursors, porous (zeosil) and nonporous (silochrome), is made to determine whether the fluorination procedure is dependent on silica porosity. Specific surface areas, measured from $N_2$ adsorption isotherms, are 150 $m^2 \cdot g^{-1}$ for silochrome and 113 $m^2 \cdot g^{-1}$ for zeosil, with pore distributions of around 40 Å. Silochrome was

* Corresponding author. E-mail: jfr@ccr.jussieu.fr.
[†] Taras Shevchenko National University.
[‡] Université Pierre et Marie Curie.
[§] E.S.P.C.I.

10.1021/jp021873d CCC: $25.00 
Published on Web 05/03/2003

**TABLE 1: Fluorination Conditions of Silochrome (SC) and Zeosil (Zs) and Sample Identification (ID)**

| sample ID | solvent and precursor used | temperature *T* (°C) and time of synthesis (h) |
|---|---|---|
| SC-W | water/silochrome | stirring for 36 h at room temperature, evaporation and calcination at 140 °C |
| SC-B | water-*tert*-butyl alcohol/silochrome | stirrring for 18 h at room temperature, evaporation and calcination at 135 °C |
| SC-A | acetonitrile/silochrome | stirring for 2 h at room temperature, at room-temperature evaporation and treatment at 70 °C |
| Zs-A | acetonitrile/zeosil | refluxing for 2 h, evaporation and calcination at 00−250 °C |
| Zs-A-F/1, Zs-A-F/2 | acetonitrile/zeosil/$CF_3COOH$ | refluxing for 2 h, evaporation and calcination at 100−250 °C |
| SC-E | ethyleneglycol/silochrome | stirring for 24 h at room temperature, evaporation and calcination at 100 °C |
| SC-P | propylenecarbonate/silochrome | stirring for 24 h at room temperature, evaporation and calcination at 100 °C |

activated at 300 °C for 8 h in an oven under air. Zeosil was activated at 400 °C for 3 h under $O_2$ and finally at 570 °C for 8 h in vacuum. Activated silicas were stored in vacuum desiccators until fluorination. Organic solvents were purified and thoroughly dried by conventional procedures.

**Fluorination Procedure.** Conditions of silica fluorination are indicated in Table 1. To the solution of 0.02 g of $NH_4F$ in 2 mL of organic solvent or an organic−water mixture was added 0.5 g of silochrome or zeosil. The slurry was stirred at room temperature or refluxed; then the solvent was evaporated, and the solid was calcined in a furnace under conditions given in Table 1. The samples were cooled to room temperature, washed with the corresponding solvent, and calcined again at 100−250 °C when needed prior to study. In two cases (preparation of Zs-A-F/1 and Zs-A-F/2), trifluoroacetic acid and zeosil were used, and the synthetic method that was applied is as follows: to the slurry of 0.5 g of zeosil in 15 mL of acetonitrile, 0.5 mL of $CF_3COOH$ and 0.02 g (Zs-A-F/1) or 0.04 g (Zs-A-F/2) of $NH_4F$ were added. The quantity of $NH_4F$ that was used is close to the equimolar Si−OH/F ratio.[8,10,11]

**Techniques. NMR Spectroscopy.** $^{19}F$ MAS NMR spectra were recorded at room temperature on a Bruker ASX300 spectrometer operating at 282.35 MHz. The spinning frequency is typically 10−14 kHz. The chemical shifts are referenced to external $C_6F_6$. Samples, as prepared or submitted to additional calcinations at 250 °C, are placed in 4-mm NMR zirconia rotors. The recycle delay of 6 s is in good agreement with fluorine spin lattice relaxation times measured for the samples.

$^{19}F \rightarrow {}^{29}Si$ and $^{1}H \rightarrow {}^{29}Si$ CP-MAS NMR spectra were recorded on Bruker ASX300 and ASX500 spectrometers operating at 59.62 and 99.35 MHz, respectively. The air-dried sample powder was placed into 4- and 7-mm zirconia rotors, respectively, that were spun at 5 kHz for all measurements. The Hartmann−Hahn conditions for $^{19}F \rightarrow {}^{29}Si$ and $^{1}H \rightarrow {}^{29}Si$ CP-MAS NMR experiments were found by replacing the sample by the rotor containing $Na_2SiF_6$ and $Q_8Me_8$, respectively. Chemical shifts are expressed using liquid TMS as an external reference. A contact time of 5 ms and recycle delay of 6 s were taken for the measurements. The number of accumulations (NS) for all experiments is given on the Figures.

**Infrared Spectroscopy.** IR spectra are recorded on a Bruker Vector 22 spectrometer. Diffuse reflectance spectra were recorded using a Harrick diffuse reflectance cell at various temperatures with a DTGS detector, an accumulation of 400 scans, a resolution of 4 $cm^{-1}$, and a KBr background. Silica samples (pure or diluted with KBr 1:4) were ground into fine powders and put into the reaction chamber without pressing. Spectra are represented in Kubelka−Munk units. Thermal in situ treatment was performed by treating samples for 1 h at the required temperatures at 0.002 Pa; then the sample was cooled to room temperature, and the spectrum was recorded.

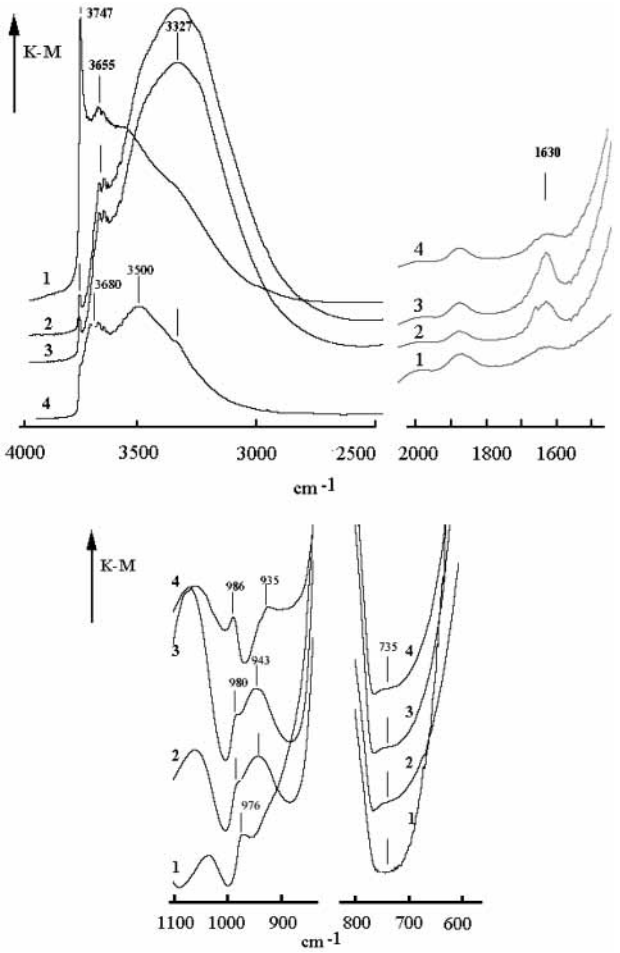


**Figure 1.** DRIFT spectra of (1**)** parent Zs in situ calcined at 250 °C under vacuum, (2) Zs-A-F noncalcined, (3**)** Zs-A-F precalcined at 250 °C, and (4) Zs-A-F precalcined at 250 °C and recalcined in situ at 100 °C under vacuum.

Thermal programmed analysis (TPD MS) was performed by heating the sample in high vacuum ($p < 10^{-3}$ Pa) at a heating rate of 0.150 °C/s. Evolving products were analyzed by mass spectrometry on a Selmi MX 7304 A instrument (Ukraine).[12] Before TPD MS measurements were made, samples were preevacuated at $10^{-3}$ Pa for 20 min.

## 3. Results and Discussion

**3.1. Infrared Results.** Fluorination was monitored by means of infrared spectroscopy. Figures 1 and 2 represent DRIFT spectra of fluorinated zeosil and silochrome samples, respectively, after the fluorination procedure and upon calcination, along with spectra of nonfluorinated precursors. Particular attention was paid to a band at 3747 $cm^{-1}$ corresponding to the stretching vibrational mode of isolated silanols and an absorption region around 980 $cm^{-1}$ where the deformational vibrational mode of isolated silanols is displayed. (The exact position of the latter depends on the silica and fluorination procedures,

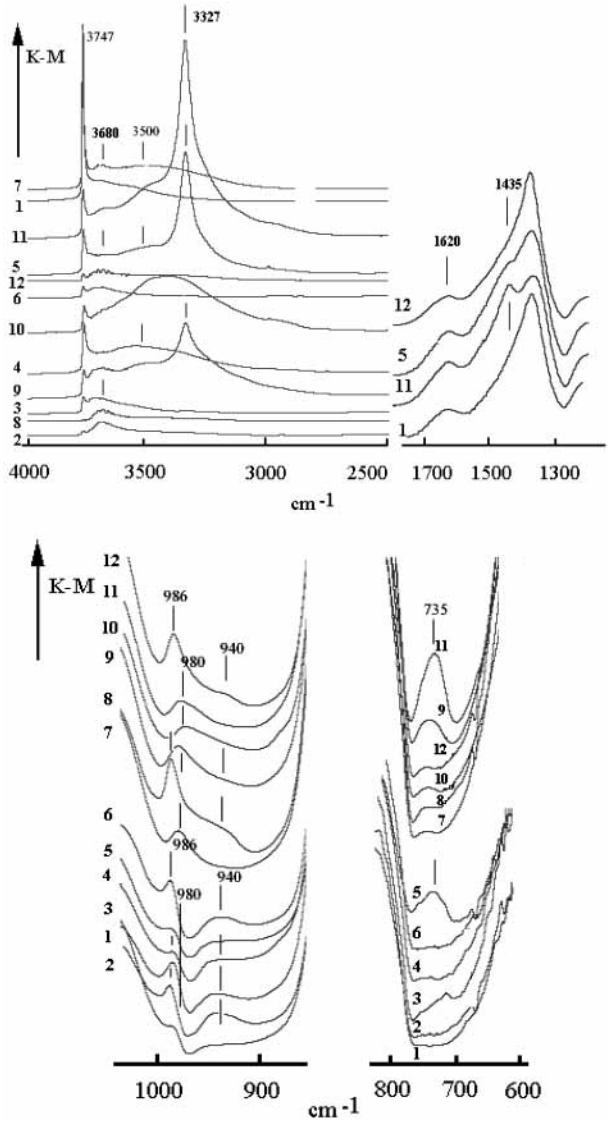


**Figure 2.** DRIFT spectra of samples in situ calcined at 250 °C under vacuum: (1) precursor SC, (2) SC-W, (3) SC-B, (4) SC-E, (5) SC-A in situ calcined at 100 °C under vacuum, and (6) SC-A. DRIFT spectra of nonvacuum samples: (7) precursor SC, (8) SC-W, (9) SC-B, (10) SC-E, (11) SC-A, and (12) SC-A precalcined at 250 °C.

which will be discussed later.[13,14]) Both bands allow us to follow the degree of silanol substitution by fluorine. The intensities of the spectra are normalized using the Si−O−Si sym vibrations at 1870 $cm^{-1}$ as an internal standard. Spectra presented in Figures 1 and 2 have nonequivalent scales.

In the spectra of nonfluorinated precursors Zs (Figure 1, spectrum 1) and SC (Figure 2, spectra 1 and 7), strong absorption was detected at 3747 $cm^{-1}$, 980 $cm^{-1}$ (Zs), and 976 $cm^{-1}$ (SC) due to isolated silanol vibrational modes, together with absorptions at 3655 $cm^{-1}$ (Zs) and 3680 $cm^{-1}$ (SC) due to hydrogen-bonded silanols. In general, fluorinated samples still exhibit the isolated silanol vibrational mode at 3747 $cm^{-1}$ (Figures 1 and 2). However, its intensity is much weaker for SC-fluorinated samples, especially for noncalcined and calcined SC-W (Figure 2, spectra 2 and 8) and calcined SC-B and SC-A (Figure 2, spectra 3 and 5) compared to the band in the spectrum of parent SC (Figure 2.1). A residual silanol absorption is detected in the spectra of fluorinated Zs (Figure 1 spectra 3 and 4), which is due to the inaccessible inner silanols.

An intense absorption at 3680 $cm^{-1}$ is detected for in situ calcined, fluorinated Zs (Figure 1, spectrum 4) and SC (Figure 2, spectra 2, 6, 9), which is smaller for nonfluorinated SC (Figure 1, spectrum 1) and Zs (Figure 2, spectra 1 and 7). This absorption in nonfluorinated samples is due to the stretching vibration of hydrogen-bonded silanols, whereas in spectra of fluorinated samples hydrogen bonded to silanols fluorine can contribute to the overall intensity and lead to an increase in this absorption. An increase in the intensity of this band becomes more obvious for calcined fluorinated Zs (compare Figure 1, spectra 3 and 4).

It is important that the intensity of hydrogen-bonded water is very low on SC-W and SC-A samples (highly fluorinated), for example, Figure 2, spectrum 12, so that no band around 3500 $cm^{-1}$ (accompanied by the bands at 1620−1640 $cm^{-1}$) is observed even without vacuum treatment. Fluorinated Si atoms easily lose hydrogen-bonded water under vacuum treatment. This can be due to the improved hydrophobicity of the fluorinated surface. Zs-A-F samples have rather high residual water absorption at 3500 $cm^{-1}$ even after calcination at 100 °C in vacuum (Figure 1, spectrum 4).

In contrast to the spectra of parent silica, the IR spectra of some fluorinated samples show a new band at 735 $cm^{-1}$ assigned to the stretching of octahedral $SiF_6^{2-}$ [5,8,9] along with the band at 3327 $cm^{-1}$ assigned to the stretching vibrational modes of the surface-adsorbed $NH_4^+$ cation (Figure 2, spectrum 11). This band is shifted compared to the band observed at 3134 $cm^{-1}$ for the free ammonium cation.[13] Simultaneous observation of the bands from $NH_4^+$ and $SiF_6^{2-}$ groups shows that the formation of $(NH_4)_2SiF_6$ takes place during fluorination when organic solvents or water are used. This coincides with what was previously reported for the fluorination in water.[8,9] We have found that the absorption intensity of $NH_4^+$ cations is already reduced by vacuum treatment at 100 °C (compare Figure 2, spectra 1 and 5). Increasing the calcination temperature to 250 °C leads to the complete decomposition of the adsorbed octahedral species, as shown by the disappearance of the bands at 3327 and 735 $cm^{-1}$ (Figure 2, spectrum 6). The octahedral species absorption is very weak for Zs-A-F/1, (Figure 1, spectra 2−4).

No further conclusion regarding the existence of the octahedral hydroxyfluorinated silicon species can be reached from IR experiments. Accordingly to Clark et al.[9] who first proposed the formation of hydroxyfluorinated species of octahedral symmetry of general formula $[F_nSi(OH)_{6-n}]^{2-}$, the same vibrational modes can be assumed for those species as for $SiF_6^{2-}$ (the band at 735 $cm^{-1}$).

Earlier, it was implied in the literature that the formation of a tetrahedral $O_3Si-F$ species leads to the absorption band coinciding with the isolated Si−OH deformational mode at 980 $cm^{-1}$,[6,8] but later investigations assign to that species an absorption at 935 $cm^{-1}$.[7] Other species that are supposed to be formed on the surface of fluorinated silica and that are characterized by defined positions in the IR spectrum are $O-SiF_3$, characterized by the band at 975 $cm^{-1}$, and the adsorption complex between HF and $O_3Si-OH$, where fluorine is coordinated to silicon, having an IR absorption at 905 $cm^{-1}$.[7] The formation of $SiF_4$ can be monitored by its vibrational modes at 800 and 1031 $cm^{-1}$.[8]

In the present work, we found for fluorinated Zs and SC several new bands in the 900−990 $cm^{-1}$ region with slightly varying positions. The Si−OH vibrational mode is located around 970 $cm^{-1}$ (Zs) and 980 $cm^{-1}$ (SC). The spectra of fluorinated Zs display a reduced Si−OH absorption band at 970 $cm^{-1}$ and a new strong absorption at 940 $cm^{-1}$, which indicates the replacement of $O_3Si-OH$ by $O_3Si-F$. After calcination, a

new band appears at 986 $cm^{-1}$ (Figure 1, spectrum 3), demonstrating that other species are formed.

The spectra of fluorinated SC depend strongly on the fluorination procedure used (Figure 2). The spectrum of SC-W does not show any visible Si−OH absorption at 980 $cm^{-1}$; however, there are new intense bands at 986 and 940 $cm^{-1}$. Calcination does not further change the spectrum. The spectra of SC-B, SC-E, and SC-A still show residual Si−OH vibration together with a new shoulder at 940 $cm^{-1}$. Calcination of these samples causes the bands at 986 and 940 $cm^{-1}$ to grow. An increase in the calcination temperature increases their intensities (compare Figure 2, spectrum 11 of noncalcined SC-A and spectrum 5 of SC-A, calcined at 100 °C, and spectrum 12 of SC-A, calcined at 250 °C). We can conclude that $O_3Si-F$ bonds are already formed at the temperatures used in the fluorination procedure (Table 1, 70−140 °C), but higher temperatures are required to advance the reaction. The spectrum of calcined fluorinated silochrome is not influenced by exposure to air, which means that the formed species are insensitive to moisture, as shown, for example, for the SC-A sample: calcined in situ under vacuum (Figure 2, spectrum 6) and previously calcined at 250 °C without vacuum (Figure 2, spectrum 12), it shows similar spectra.

The increase in the intensity of the bands at 940 $cm^{-1}$ on calcination together with the decreasing intensity of the $SiF_6^{2-}$ vibration at 735 $cm^{-1}$ implies that the additional isolated tetrahedral species $O_3Si-F$ are formed upon thermal treatment, presumably from octahedral fluoro or hydroxyfluoro species. As shown by Duke et al.,[9] decomposition of surface-adsorbed $SiF_6^{2-}$ is likely to lead to the formation of $SiF_4$. However, its vibrational modes are to be observed at 800 and 1031 $cm^{-1}$, but these are found neither by the authors nor in this work. On the contrary, the band at 986 $cm^{-1}$ that was newly observed on fluorinated silica can plausibly correspond to other fluorinated species ($O_2SiF_2$ and $O-SiF_3$) that are newly formed upon the decomposition of octahedral species $O_2SiF_2$ and $O-SiF_3$. This value is closest to the Si−F vibration in $O-SiF_3$ at 978 $cm^{-1}$. Indeed, decomposing hydroxyfluorinated and hexafluorosilicate species produce $SiF_4$, and its interaction with silica leads to the secondary fluorination process, generating additional $O_3Si-F$ and $O-SiF_3$ groups.

The IR data reported here suggest that the treatment of silochrome with organic, mixed water−organic, or an aqueous solution of $NH_4F$ leads to the formation of both tetrahedral $O_3Si-F$ and octahedral $(SiF_6)^{2-}$ species at low temperatures. We did not see any noticeable formation of $SiF_6^{2-}$ on water-fluorinated samples compared to previously reported data,[6,8] indicating that $(NH_4)_2SiF_6$ is easily desorbed if the sample is washed with water after the synthesis. The use of a water−*tert*-butyl alcohol mixture results in a decreased number of isolated $O_3Si-F$ groups compared to using an aqueous solution, together with the increased number of octahedral species. Fluorination in ethyleneglycol does not result in the evident formation of $O_3Si-F$. When fluorination is performed in acetonitrile, the greatest intensity of both $O_3Si-F$ and $SiF_6^{2-}$ is detected. The use of $CF_3COOH$ in acetonitrile reduces the formation of octahedral species and also remarkably favors the formation of tetrahedral $O_3Si-F$. Postsynthetic calcination induces the decomposition of octahedral fluorinated species and promotes $O_3Si-F$ formation, presumably via secondary fluorination by $SiF_4$.

**3.2. Thermal Decomposition of Fluorinated Silica Followed by Mass Spectrometry.** The results of thermal desorption experiments, followed by mass spectrometry, are presented in Figures 3 and 4. It can be seen from Figure 3 that the fluorination of SC changes its affinity to water. The thermal desorption of water (peaks with *m*/*z* 18, 17) from a nonfluorinated SC surface proceeds in three steps—at 70−120 °C, at 250−350 °C, and above 650 °C—that are attributed to dehydration (physically adsorbed and hydrogen-bonded water) and dehydroxylation, respectively.[1] A comparison of curves 1 and 3 shows that only physically adsorbed water is present on SC-A (desorption peak at 80 °C), and no desorption of hydrogen-bonded water and hydroxyl condensation was detected. For SC-P, the main peak of water desorption occurs at a higher temperature than for pure silochrome, with a maximum at 350 °C. The absence of a hydroxyl condensation peak at 600 °C suggests that there are almost no isolated silanols left on the surface of fluorinated samples SC-A and SC-P. We assume that the hydroxyls left on the fluorinated surface are mostly a constituent part of the hydroxyfluorosilicon species. Part of the hydroxyls that are detected could also be due to the internal silica hydroxyls that are inaccessible for chemical modification.

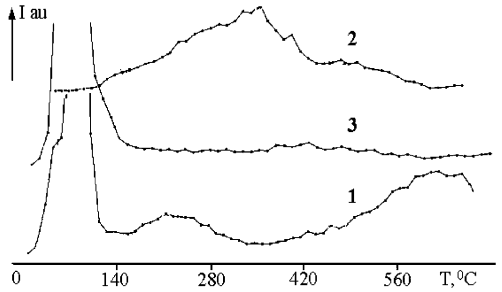


**Figure 3.** Thermal desorption of water from (1) SC, (2) SC-A, and (3) SC-P.

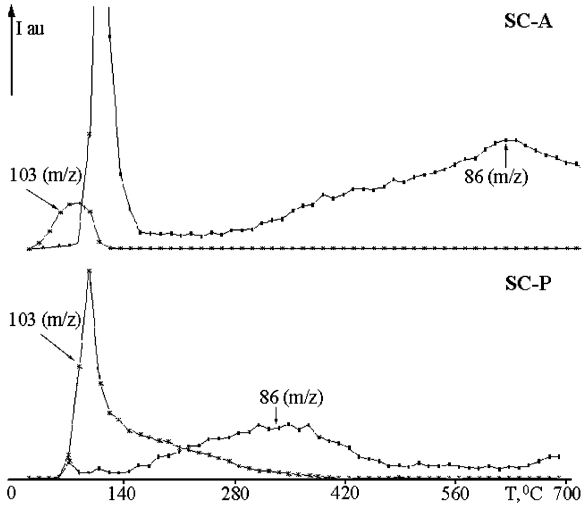


**Figure 4.** Programmed thermal desorption of surface-bonded fluorinated groups from SC-A and SC-P samples followed by TPD-MS.

As previously reported,[9] during the thermal treatment of silica fluorinated in water with $NH_4F$, the desorption of $NH_3$ occurs at 100−200 °C, and the main weight loss occurs at 250−300 °C, being assigned to the loss of hydroxofluorosilicates. The process of the thermal decomposition of fluorinated silochrome (followed mass spectrometrically) observed in this work is in agreement with that reported for water-fluorinated silica; however, there are several differences between the SC-A and SC-P samples (Figure 4). Various silicon- and fluorine-containing species were evolved during the thermal decomposition of SC-A and SC-P. Species that were assigned to $SiF_3^+$ (*m*/*z* 85, accompanied by the peak with *m*/*z* 86 assigned to $SiF_3H^+$) and $SiF_3OH_2^+$ (*m*/*z* 103, accompanied by three peaks

with *m*/*z* 102, 101, and 104 assigned to $SiF_3OH^+$, $SiF_3O^+$, and $SiF_4^+$, respectively) predominate in the mass spectra, the contribution of other high-weight silicon-containing species being negligible. The existence of the species with *m*/*z* 101, 102, and 103 was assigned to the protonation pattern rather than to the silicon isotope distribution ($^{28}Si$, $^{29}Si$, $^{30}Si$) on the basis of the peak intensity ratios. All of these peaks are accompanied by peaks with *m*/*z* 20 and 19 assigned to $HF^+$ and $F^+$, respectively.

The main decomposition of fluorinated species from the surface of SC-A and the desorption of $SiF_3^+$ and $HSiF_3^+$ (*m*/*z* 85 and 86, respectively) take place at 140 °C. At this temperature, the surface loses initially formed, adsorbed octahedral fluorinated species $(NH_4)_2SiF_6$, presumably in the form of $SiF_4$. This process is supported by data from DRIFT and seems to be general for SC and Zs fluorinated in aqueous or organic media. The evolution of the weak peak assigned to $SiF_3OH_2^+$ (*m*/*z* 103) is observed at 80 °C, corresponding to the decomposition of hydroxyfluorinated species. Other species are formed at higher temperatures with a maximum above 600 °C and are evolved as $SiF_3^+$ and $SiF_3H^+$.

On the contrary, at low temperature, the surface of SC-P loses mainly hydroxyfluorides, detected as the growing peaks of $SiF_3OH_2^+$ (*m*/*z* 103), accompanied by peaks of $SiF_3OH^+$ (*m*/*z* 102) and a weak peak of $SiF_3O^+$ (*m*/*z* 101). At the same time, the evolution of $SiF_4^+$ with *m*/*z* 104 occurs. Above 250 °C, the evolution of $SiF_3^+$ and $SiF_3H^+$ (*m*/*z* 85 and 86, respectively) prevails (Figure 4). The simultaneous evolution of the $SiF_3^+$ and $SiF_3H^+$ species and water (Figures 3 and 4) allows us to propose that these peaks also reflect the decomposition of octahedral hydroxyfluorosilicon ($SiF_nOH_{6-n}$) surface species. This process of SC-P decomposition is consistent with that reported for water-fluorinated silica.[8,9]

Therefore, we come to the conclusion that fluorination in propylene carbonate (SC-P), apart from the formation of tetrahedral $O_3Si-F$ species, leads to the formation of large numbers of hydroxyfluorinated species. The use of acetonitrile (SC-A) results in a higher conversion of silanols to octahedral silicon fluoride. Further evolution of $SiF_3^+$ from the surface of fluorinated silica detected at higher temperatures (400−660 °C) is assumed to be due to the migration of fluorine of tetrahedral mono (bi-) fluorinated species over siloxane bonds and the condensation to $SiF_4$. This process may be analogous to silanol condensation on bulk silica, which is also implied by its occurrence in a similar temperature range.

**3.3. NMR Results. 3.3.1. $^{19}F$ MAS NMR.** According to the literature,[5,8,15] the formation of fully substituted octahedral $SiF_6^{2-}$ anions for KF-fluorinated silica is revealed in $^{19}F$ NMR spectra by the peak at 34−35 ppm. This is also found for silica fluorinated with $NH_4F$ in water by Clark et al.[9] This peak exhibits relatively high symmetry as a result of the mobility and symmetry of $SiF_6^{2-}$ anions. Earlier it was indicated that NMR spectroscopy could not identify the chemically bound surface ≡Si−F of tetrahedral symmetry because of its high chemical shift anisotropy.[15] The review of Miller et al.[16] summarizes the latest data on fluorinated silica. The chemical shift for adsorbed $(NH_4)_2SiF_6$ is usually observed around 34 ppm, whereas that of anion $(SiF_6)^{2-}$ varies more depending on the cation associated with $(SiF_6)^{2-}$ and the nature of the support. The fluorine chemical shift in tetrahedral $O_3Si-F$ has not yet been determined. However, different values of the fluorine chemical shift were reported for the Si−F bond in $Na_2SiF_6$. These values are scattered between 10 and 27 ppm.[17−19]

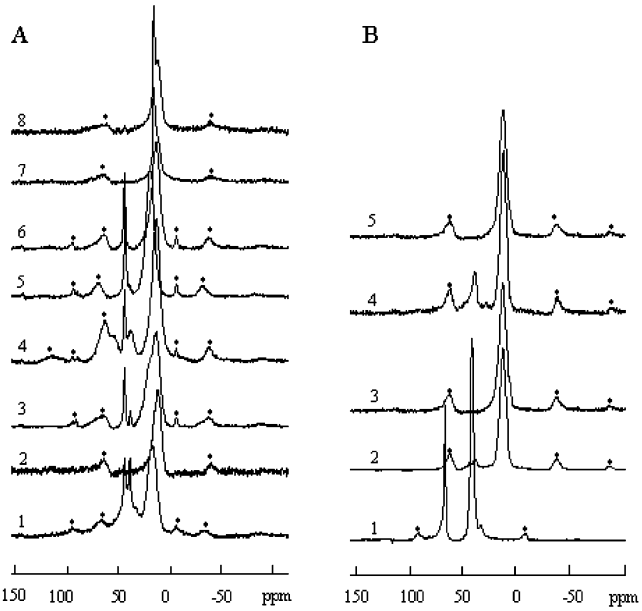


**Figure 5.** (A) $^{19}F$ MAS NMR spectra of fluorinated (1) SC-A, (2) SC-A calcined at 250 °C in vacuum for 24 h, (3) Zs-A-F/1, (4) Zs-A-F/1 calcined at 250 °C in vacuum for 24 h, (5) Zs-A-F/2, (6) Zs-A-F/2 calcined at 250 °C in vacuum for 24 h, (7) SC-E, and (8) SC-E calcined at 250 °C in vacuum for 24 h. (B) $^{19}F$ MAS NMR spectra of (1) $NH_4F$ mechanically mixed with silochrome, (2) SC-W, (3) SC-W calcined in vacuum at 135 °C for 24 h, (4) SC-B, and (5) SC-B calcined in vacuum at 135 °C for 24 h. (*) indicates side spinning bands.

**TABLE 2: $^{19}F$ Chemical Shifts for Fluorinated SC and Zs**

| sample ID | | chemical shift, ppm of $C_6F_6$: reagent free or adsorbed | chemical shift, ppm of $C_6F_6$: octahedral and tetrahedral species |
|---|---|---|---|
| $NH_4F$ | | 82.9 | |
| $NH_4F-Si$ mixture | | 66.1−67.0 (doublet); 41.5 | 34.0 |
| SC−W | noncalcined | 43.5 (weak) | 38.0 (weak); 14.0 |
| | calcined | | 12.0 |
| SC−B | noncalcined | 43.5 | 38.0; 12.0 |
| | calcined | | 11.0; 5.0 |
| SC-A | noncalcined | 43.0 | 37.0; 29.0; 20.0 |
| | calcined | | 18.0; 12.0 |
| SC-E | noncalcined | | 15.0; 11.0 |
| | calcined | | 15.0; 11.0 |
| Zs-A−F/1 | noncalcined | 43.0 | 38.0; 28.0; 12.0 |
| | calcined | 43.0 | 38.0; 12.0 |
| Zs-A−F/2 | noncalcined | 43.0 | 38.0 (weak); 28.0 |
| | calcined | 43.0 | 12.0 |

$^{19}F$ MAS NMR spectra of the fluorinated samples are presented in Figure 5. The observed chemical shifts of the samples are given in Table 2.

The $^{19}F$ MAS NMR spectrum of the solid undiluted ammonium fluoride $NH_4F$, which was used as a precursor, exhibits a single peak at 82.9 ppm. To determine whether dilution with silochrome influences the chemical shift of ammonium fluoride, a mixture with about 70 wt % silochrome was prepared by grinding it in the mortar directly before use. The spectrum of the resulting sample (Figure 5.B-1) contains three peaks of different intensities: doublets at 66−67, 41.5, and 34 ppm. The absence of the peak corresponding to undiluted ammonium fluoride means that mechanical mixing leads to strong contact between ammonium fluoride and the silochrome. This can consist of the adsorption of $NH_4F$ on the surface. The existence of the three different peaks can be explained by the presence of different types of interactions of $NH_4F$ species with the

surface. The narrow doublet at 66−67 ppm is very close to the position of the peak of the parent $NH_4F$. Its small line width may reflect a high mobility of the corresponding species. Therefore, we assign this to a weakly interacting $NH_4F$ species, coordinated via $NH_4^+$. The resonance line at 41.5 ppm can be tentatively assigned to more strongly interacting $NH_4F$, adsorbed to the silicon atom via F. The weak peak at 34 ppm indicates that $(NH_4)_2SiF_6$ is also formed in the mixture.

The spectra of most fluorinated samples studied in this work exhibited three peaks (Figure 5) at 43.5 ppm and near 32−38 and 11−29 ppm.

The moderate or weak peak at 43.5 ppm corresponds to adsorbed $NH_4F$, according to the spectrum recorded for the silochrome−$NH_4F$ mixture. A rather weak peak at 32−38 ppm reflects the presence of $SiF_6^{2-}$ species adsorbed on silica. The varying position of this peak can be explained by the possibility of the formation of a large variety of hydroxy species with the general formula $[(OH)_nSiF_{6-n}]^{2-}$. We argue that the high-field peaks can result in particular from the fluorinated hydroxysilicon species of octahedral symmetry because the fluorine chemical shift is close to that of the $SiF_6^{2-}$ species.

The strongly asymmetric broad peak, whose position varies between 11 and 29 ppm depending on the method of fluorination, has not been previously reported for $NH_4F$-fluorinated silica. However, these values of the chemical shift are very close to that observed for the F group in $Na_2SiF_6$. The position of this peak varies with the method of fluorination. Moreover, a dramatic change in its shape occurs upon thermal treatment so that it becomes narrower and shifts to high field, to about 11−12 ppm. Correlation between the treatment temperature of the samples and the position and shape of the NMR peaks, together with an analysis of the DRIFT spectra, allows the tentative assignment of the peak at 11 ppm to the tetrahedral fluorinated silicon species $O_3Si-F$. This peak was not observed by the authors of ref 9. This is probably due to the prevalence of the peak at 34 ppm and the low spinning frequency (4 kHz), which could cause this peak to be hidden by the spinning sidebands.

The broadness of peaks can result from the high chemical-shift anisotropy and residual $^{19}F-^{19}F$ and $^{19}F-^{1}H$ dipole coupling, which cannot be completely averaged at the spinning frequency used. To completely average this dipole coupling, a spinning frequency higher than 30 kHz may be necessary, as previously indicated in ref 15. The large line width of the $^{19}F$ peaks in the 11−29 ppm range could be explained by heteronuclear dipole coupling. Therefore, it implies the close proximity of fluorine to the neighboring silanols. This corresponds well to our assignment of these lines to hydroxyfluorinated species with general formula $[(OH)_nSiF_{6-n}]^{2-}$ and lattice-bonded $(SiO)_xSi(OH)_yF_z$.

In light of these results and those of the FTIR and TPD MS studies, the shift of the signal around 11−28 ppm to 11 ppm may result from the thermal decomposition of hydroxofluorinated species to more stable fluorinated tetrahedral $O_3Si-F$. Moreover, in the spectra of calcined samples, the line at 11 ppm is often accompanied by a shoulder at 15−18 ppm. This shoulder may be due to $O_2Si-F(OH)$. However, we do not exclude the possibility that geminal $O_2SiF_2$ or $O-SiF_3$ species are formed because their resonance lines may be at the same position as that of $O_3Si-F$. In the spectrum of SC-E, peaks at 11 and 15 ppm were detected, and they were better resolved after the calcination. This can be due to the narrowing of the lines because of the elimination of silanols constituting hydroxyfluoro species.

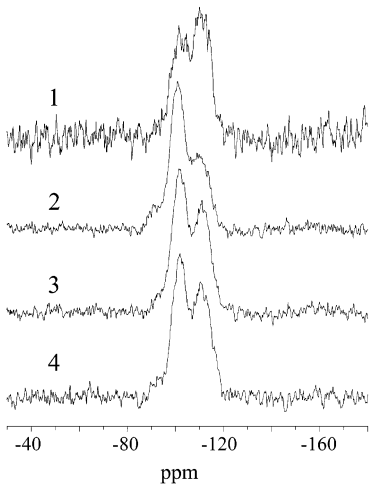


**Figure 6.** $^{1}H \rightarrow {}^{29}Si$ CP-MAS NMR spectra of air-dried fluorinated samples: (1) SC-W (NS = 19 067), (2) SC-E (NS = 2626), (3) Zs-A-F/1 calcined at 250 °C (NS = 4000), and (4) Zs-A-F/1 (NS = 11 725).

The peaks due to the fully fluorinated octahedral silicon (38 ppm) were weak compared to those of the hydroxy species and $O_3Si-F$ (11−28 ppm). The relative concentration of these species depends markedly on the fluorination method and subsequent thermal treatment. For silochrome fluorinated in an organic solvent or water, the intensities of the peaks between 43 and 34 ppm decrease considerably upon heating, and the peaks disappear completely for the samples calcined at 250 °C in vacuum for 24 h. This coincides with the IR-detected decomposition of octahedral fluorinated anions and ammonia desorption. For the samples based on zeosil (Zs-A-F/1, Zs-A-F/2), different changes are caused by the thermal treatment. The spectra exhibit a broad line at 20−28 ppm, which is similar to that of fluorinated silochrome, that shifts upon calcination to 12 ppm. However, both peaks at 43 ppm (Zs-A-F/1, Zs-A-F/2) and 37 ppm (Zs-A-F) are still observed in the spectra of calcined samples. The slow desorption of fluorinated species, limited by diffusion, was also observed in the FTIR spectra. A small reduction in the S/N ratio was observed for calcined samples, which agrees with the loss of fluorine upon heating. Comparing the various fluorination procedures shows that fluorination in water and ethylene glycol results in a negligible formation of silicon hexafluoride, but the addition of *t*-BuOH favors this compound. Fluorination in acetonitrile leads to more $SiF_6^{2-}$. The low S/N ratio for SC-E, compared to that of the other samples, could be due to the lower fluorine content.

Similar NMR results for the fluorination of zeolites have been reported by Sanches et al.[20] The presence of two resonance lines at 22 and 32 ppm in the $^{19}F$ spectra has been noticed. 2-D $^{29}Si\{^{19}F\}$ HetCor-MAS experiments allowed the authors to correlate these lines with the $^{29}Si$ peak of framework silicon at −104 ppm. Therefore, these $^{19}F$ peaks were attributed to fluorine bound to framework silicon. A set of sharp and broad signals was also found between 10 and 18 ppm but was in this case assigned to fluorinated nonframework aluminum hydroxy complexes.

**3.3.2. $^{19}F \rightarrow {}^{29}Si$ CP-MAS and $^{1}H \rightarrow {}^{29}Si$ CP-MAS NMR.** To understand the nature and structure of fluorinated silicon species better, $^{19}F \rightarrow {}^{29}Si$ and $^{1}H \rightarrow {}^{29}Si$ CP-MAS NMR measurements were performed on some fluorinated silicas. The obtained spectra are represented in Figures 6 and 7, respectively. The $^{1}H \rightarrow {}^{29}Si$ CP-MAS spectra are similar to those reported for fumed and precipitation silica, respectively.[21] One can

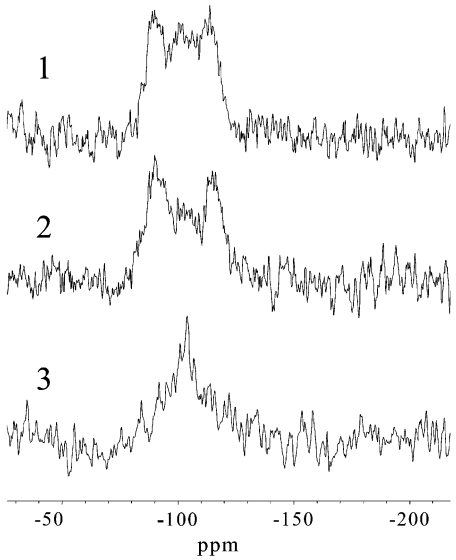


**Figure 7.** $^{19}F \rightarrow {}^{29}Si$ CP-MAS NMR spectra of (1) SC-W (NS = 18 800), (2) Zs-A-F/1 (NS = 10 800), and (3) Zs-A-F/1 calcined at 250 °C (NS = 8324).

distinguish between isolated silanols ($Q_3$ = SiOH) at −103 ppm, bulk silicon ($Q_4$ = $SiO_2$) at −112 ppm, and a weak peak of geminal surface silanols ($Q_2$ = $Si(OH)_2$) at −92 ppm. The spectra of SC-A before and after calcination, SC-W, and SC-E are similar except for the ratio between peaks of different Q species in each spectrum. This change is due to variations of the relative amounts of different Q species from one sample to another. For SC-E, a comparison of the relative intensity of the different peaks indicates the highest proportion of isolated silanols, in accordance with the lowest degree of fluorination. The relatively low signal/noise ratio of the $^{29}Si\{^1H\}$ CP MAS spectrum of the SC-W may be due to its having the highest degree of fluorination (low proton content).

$^{19}F \rightarrow {}^{29}Si$ CP-MAS NMR spectra (Figure 7) of fluorinated samples are found to be much more dependent on the solvent used for the fluorination and on the thermal treatment. The spectra of both SC-W and Zs-A-F/1, noncalcined, exhibit three peaks at approximately the same positions as those observed for Q species: −94, −104, and −113 ppm. After calcination, fluorinated Zs-A-F/1 silica shows a single broad peak at approximately −104 ppm. Moreover, the peak corresponding to the octahedral hexafluorosilicate anion ($SiF_6^{2-}$), which was reported at −186 ppm,[8] was not observed for any of the samples studied in this work, similar to the data reported in ref 9. This could be explained by its relatively low concentration (for an $CH_3CN$ sample) or absence (for a $H_2O$ sample) on the fluorinated surface, as was previously seen in the DRIFT and $^{19}F$ NMR spectra. Under the same experimental conditions, no signal was detected for the SC-E sample, even for 8894 scans. This may be due to its low degree of fluorination, which was observed earlier in the $^{19}F$ spectra (Figure 5A, spectrum 8).

It was reported that the $^{29}Si$ chemical shift of tetrahedral $O_3$-Si−F should be very close to that of bulk silica.[22] The silicon chemical shift in $(SiO)_3$−Si−F has been calculated by Clark et al.[9] on the basis of the group electronegativity approach proposed by Janes et al.[23] A value of −107.3 ppm was found. This value is very close to that measured in this work for the noncalcined and calcined fluorinated sample Zs-A-F/1, −104 ppm (Figure 7). Therefore, this peak is attributed to $(SiO)_3$−Si−F. A similar chemical-shift value for fluorinated silicon was also found for fluorinated zeolites in ref 20.

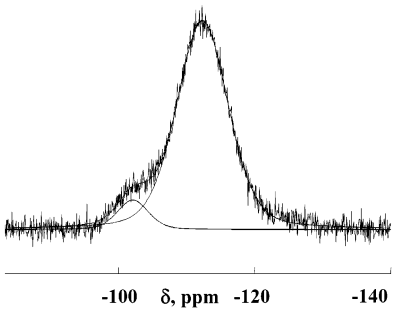


**Figure 8.** $^{29}Si$ MAS NMR spectrum of the Zs-A-F/1 sample calcined at 250 °C (NS = 2400, interpulse delay of 30 s).

In the spectra of noncalcined samples, additional strong peaks are present at −94 and −114 ppm. We suggest that the former can arise from the hydroxyfluorinated silicon species of tetrahedral geometry. Using Janes' approach, we calculated the chemical shift of various fluorinated silicon species that could be expected to exist on the surface. The values that were obtained are −97.9, −97.2, and −88.4 ppm for the species of formulas $(SiO)_2(OH)Si-F$, $(SiO)_2SiF_2$, and $OSi(OH)F_2$, respectively. All of these values are very close to the position of the peak (−94 ppm) of the $^{19}F \rightarrow {}^{29}Si$ CP-MAS spectra of the uncalcined samples (Figure 7, spectra 1 and 2). Consequently, we assume that the peak at −94 ppm is due to both types of silicon species: $(SiO)_2(OH)Si-F$ and $(SiO)_2SiF_2$, the existence of the third species being unlikely.

The attribution of the peaks is confirmed by the influence of calcination on the $^{19}F$ and $^{19}F \rightarrow {}^{29}Si$ CP-MAS NMR spectra of sample Zs-A-F/2. Calcination induces the reduction of the relative intensity of the $^{29}Si$ peak at −94 ppm (Figure 8, spectra 2 and 3) and the shift of the $^{19}F$ peak from 28 to 12 ppm (Figure 6, spectra 5 and 6). Spectra of the calcined sample contain peaks at 12 ppm ($^{19}F$) and −104 ppm ($^{29}Si$) arising from the most thermally stable species, presumably $O_3Si-F$. This correlates with our previous assignments of these fluorine and silicon peaks. Consequently, one can propose that the signals in the spectrum of the noncalcined sample ($^{29}Si$ peak at −94 ppm and that of $^{19}F$ at 28 ppm) can be attributed to the less thermally stable species $(SiO)_2(OH)Si-F$ or $(SiO)_2Si-F_2$.

On the basis of the Janes equation,[22] the peak observed in the $^{19}F \rightarrow {}^{29}Si$ CP-MAS NMR spectra of noncalcined fluorinated silica at −114 ppm cannot be assigned to any fluorine-containing species. Calculating the chemical shifts using Janes' electronegativity approach indicates that this signal can arise only from nonfluorinated silicon species. Most plausibly, this peak arises from the bulk silicon, which is detected under $^{19}F \rightarrow {}^{29}Si$ cross-polarization experimental conditions due to the space interaction. It can be seen (Figure 7, spectra 2 and 3) that its intensity is markedly decreased by calcination. This can be due to the loss of fluorine (as shown before by TPD MS experiments in the form of $SiF_4$ and $SiF_3OH$), resulting in a lower amount of fluorine contributing to polarization transfer. To verify this observation, the silicon spectrum of the Zs-A-F/1 sample calcined at 250 °C was measured by direct observation ($^{29}Si$ MAS NMR spectrum, represented in Figure 8). Using the Gauss−Lorenz simulations, the spectrum can be decomposed into two peaks: one at −102 ppm (8% of the total intensity) and one at −112 ppm (92% of the total intensity). We assume that the former peak represents both $O_3Si-OH$ and $O_3Si-F$ species and that the latter one represents bulk silicon. It is obvious that under these experimental conditions the proportion of signal from bulk silicon is much higher than that from surface silicon species $O_3Si-OH$ and $O_3Si-F$.

**SCHEME 1: Possible Mechanism of Initial $NH_4F$ Interaction with the Silica Surface**

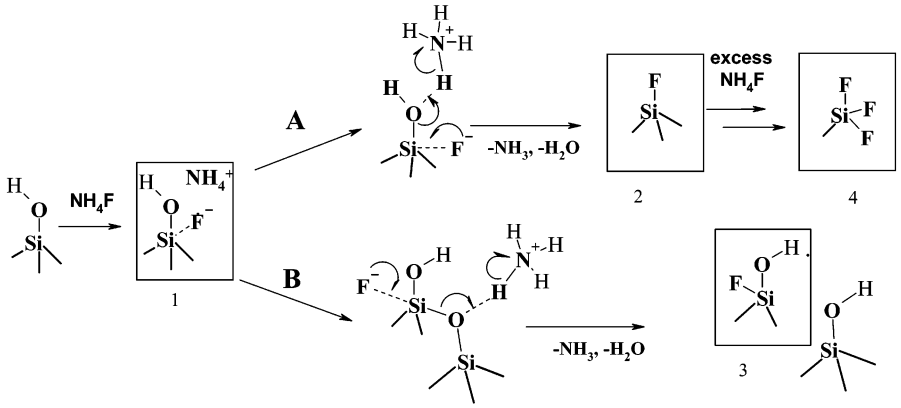


**SCHEME 2: Possible Mechanisms for the Decomposition of Fluorinated Silica**

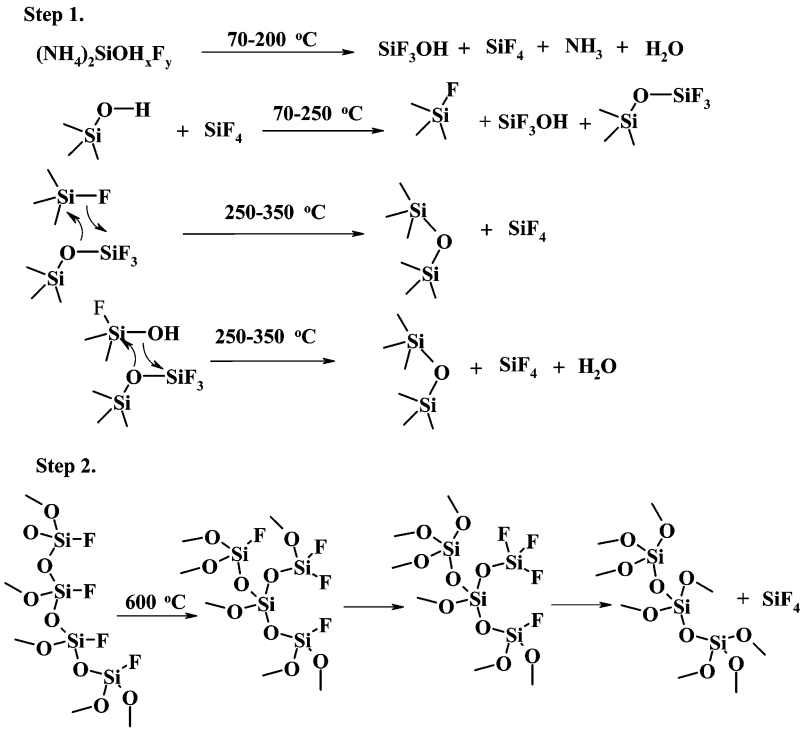


## Discussion and Conclusions

Treating silica with $NH_4F$ in organic or aqueous media leads to the formation of various species of tetrahedral and octahedral geometry. According to the $^{19}F$ NMR data, we propose that fluorination proceeds first via $NH_4F$ adsorption on the surface and the formation of coordination complex **1** (Scheme 1).

Transformations of this complex occur at room temperature and can proceed in two main directions (marked on the Scheme as A and B): nucleophilic substitution of hydroxyl, A, and fluorinative opening of the siloxane bridge, B. The first way leads to the formation of surface-bound tetrahedral $O_3Si-F$ species **2**, whereas the second gives hydroxyfluorinated silicon $O_2Si(OH)F$ **3**. Mild thermal treatment accelerates the fluorination processes, ammonia and water being eliminated. An excess of the fluorination reagent, (Scheme 1, A) may lead to the further transformation of species **2** to species **4** ($O-SiF_3$), which was observed by IR spectroscopy. This "excessive" fluorination is facilitated upon the introduction of each subsequent fluorine atom to silicon as a result of the increase in the relative positive charge on silicon.

Furthermore, as a result of this excessive fluorination, part of the silicon can be detached from the surface in the form of hydroxyfluorinated octahedral $(SiF_{6-x}OH_x)^{2-}$ and fully fluorinated $SiF_6^{2-}$ species. Their decomposition upon calcination probably gives rise to new highly reactive species—$SiF_4$, for example—

that can participate in secondary fluorination processes, yielding additional $O_3Si-F$ and $-SiF_3$:

$$(NH_4)_2SiF_6,\ (NH_4)_2(SiF_{6-x}OH_x) \rightarrow SiF_4 + H_2O + NH_3$$

This explains the increase in the intensity of the bands in the IR spectra assigned to vibrations of $Si-F$ and $-SiF_3$ groups upon calcination at 250 °C.

The processes occurring on the fluorinated surface at different treatment temperatures can be represented by Scheme 2.

A mass spectrometry analysis of the species evolved from the fluorinated surface at different temperatures shows that the decomposition proceeds in two steps. The first step occurs at temperatures of 70−200 °C and includes the decomposition of initially formed octahedral species and hydroxyfluorinated

species, eliminated mainly as $SiF_4$ ($SiF_3^+$ peak), $SiF_3OH$ ($SiF_3O^+$, $SiF_3OH^+$, $SiF_3OH_2^+$ peaks), water, and ammonia. Further elimination of $SiF_4$ (250−350 °C) is probably due to the condensation of $O-SiF_3$ with $O_3Si-F$. The second step requires much higher temperatures (>600 °C) and consists of the migration of the isolated ≡Si−F over siloxanes, new siloxane formation, and the elimination of $SiF_4$. This process may be similar to silanol condensation on bulk silica, which is known to take place in a similar temperature range.

The thermal desorption of water, namely, the absence of a hydroxyl condensation peak at 600 °C, shows that the majority of the silanols on the silochrome surface are replaced by Si−F groups after low-temperature fluorination with $NH_4F$. The affinity of the fluorinated surface toward water is strongly diminished: dehydration takes place at low temperatures, showing that the fluorinated silica is hydrophobic.

The process of surface fluorination is found to be influenced by the nature of the solvent. Thus, an enhanced formation of octahedral fluorinated species and undesirable surface erosion are observed in acetonitrile. When carried out in water, a water−butanol mixture, and propylene carbonate, fluorination is likely to yield tetrahedral ≡Si−F and $SiF_xOH_y$ species. Ethyleneglycol is found to be an inferior solvent because of the low overall fluorination yield. We assume that some silanols left on the surface after fluorination are a constituent part of ($SiF_xOH_y$) species. Part of the hydroxyls detected by spectroscopic techniques could be due to the internal silica hydroxyls, which are inaccessible for chemical modification. A more complete substitution of silanols with fluorine is observed for the pyrogenic silica, silochrome, than for the precipitation silica, zeosil. Greater numbers of inner silanols of the latter were inaccessible for modification under the conditions applied. The desorption of ammonia and fluoro species formed during the decomposition of the fluorinated surface is also slow on zeosil.

**Acknowledgment.** We are grateful for financial support from the NATO SfP Program 971896 and INTAS Grant 97-1116 “Solid superacids”.

## References and Notes

(1) *Covalently Modified Silica in Adsorption, Catalysis and Chromatography*; Lisitchkin, G. V., Ed.; Khimija: Moskva, Russia, 1986.

(2) Zaitsev, V. N. *Complexing Silicas: Synthesis, structure of bonded layer and surface chemistry*; Folio: Kharkov, 1997.

(3) Bossaert, W. D.; De Vosq, D. E.; Van Rhijn, W. M.; Bullen, J.; Grobet, P. J.; Jacobs, P. A. *J. Catal.* **1999**, *182*, 156.

(4) Katsuo, T.; Satohito, Y. and Kimio, T., *Bull. Jpn. Pet. Inst.* **1970**, *12*, 136.

(5) Iler, R. K. *The Chemistry of Silica*; Wiley: New York, 1979.

(6) In *Chemically Modified Surfaces: Recent Developments;* Pesek, J. J., Matyska, M. T., Abuelafiya, R. R., Eds.; Royal Society of Chemistry: Cambridge, U.K., 1996.

(7) Voronin, E. F.; Chuiko, A. A. In *Chemistry of the Silica Surface*; Naykova dymka: Kiev, 2001.

(8) Duke, C.; Miller, J.; Clark, J.; Kybett, A. *Spectrochim. Acta, Part A* **1990**, *46*, 1381.

(9) Clark, J. H.; Kybett, A. P.; Piers, A. S.; Williamson, C.; Miller, J. M. In *Chemically Modified Surfaces: Proceedings of the Fourth Symposium on Chemically Modified Surfaces*; Chadds Ford, PA, July 31−August 2, 1991; Mottola, H. A., Steinmetz, J. R., Eds.; Elsevier Science: Amsterdam, 1992; pp 193−207.

(10) Zhuravlev, L. T. *Langmuir* **1987**, *3*, 316.

(11) Mathias, J.; Wannemacher, G. *J. Colloid Interface Sci.* **1988**, *125*, 61.

(12) Pokrovsky, V. A. *Adv. Sci. Technol.* **1996**, *14*, 301.

(13) Socrates, G. *Infrared Characteristic Group Frequencies*; Wiley-Interscience: Chichester, U.K., 1980.

(14) Hair, M. *Infrared Spectroscopy in Surface Chemistry*; Marcel Dekker: New York, 1967.

(15) Harris, R. K.; Jackson, P. *Chem. Rev.* **1991**, *91*, 1427.

(16) Miller, J. M. *Prog. Nucl. Magn. Reson. Spectrosc.* **1996**, *28*, 255.

(17) Hayashi, S.; Hayamizu, K. *Bull. Chem. Soc. Jpn.* **1990**, *63*, 913.

(18) Burum, D. P.; Elleman, D. D.; Rhim, W. K. *J. Chem. Phys.* **1978**, *68*, 1164.

(19) Shaler, T.; Dingwell, D. B.; Keppler, H.; Kneller, W.; Merwin, L.; Sebald, A. *Geochim. Cosmochim. Acta* **1992**, *56*, 701.

(20) Sanches, N. A.; Saniger, J. M.; d’Espinose de la Caillerie, J.-B.; Blumenfeld, A.; Fripiat, J. J. *J. Catal.* **2001**, *201*, 80.

(21) Legrand, A. P.; Homel, H.; Doremieux, C.; d’Espinose de la Callierie, J.-B. In *The Surface Properties of Silicas*; Legrand, A. P., Eds.; Wiley and Sons: Chichester, U.K., 1998; pp 235−285.

(22) Janes, N.; Oldfield, E. *J. Am. Chem. Soc.* **1985**, *107*, 6769.

(23) Janes, N. K.; Mann, B. E. In *NMR and the Periodic Table*; Harris, R. K., Mann, B. E., Eds.; Academic Press, London, 1978.